Case Studies in Construction Materials 13 (2020) e00446

Contents lists available at ScienceDirect

Case Studies in Construction Materials

journal homepage: www.elsevier.com/locate/cscm

Short communication

Evaluating the interaction between engineered materials and aircraft tyres as arresting systems in landing overrun events

Misagh Ketabdari[a,*], Emanuele Toraldo[a], Maurizio Crispino[a], Vardhman Lunkar[b]

[a] Transportation Infrastructures and Geosciences Section, Department of Civil and Environmental Engineering, Politecnico di Milano, 20133, Milan, Italy
[b] TRASPOL-Research Center on Transport Policy, Politecnico di Milano, 20133, Milan, Italy

ARTICLE INFO

Article history:
Received 9 March 2020
Received in revised form 31 August 2020
Accepted 7 October 2020

Keywords:
Runway overrun
Engineered materials arresting system
Runway end safety area
Aviation risk contour map

ABSTRACT

According to the registered databases of air accidents around the world, landing overruns are the most probable accidents among all runway excursion events. Although new aircraft are enhanced with the latest technologies that improve the maneuvers safety, the frequency of landing overruns are bound to increase because of the ascending growth rate of annual traffic. The principal scope of this paper is to evaluate the functionality of Engineered Materials Arresting System (EMAS) as a mitigation strategy to reduce the possible consequences of landing overrun events and in particular to determine if installing an EMAS can help land-locked airports to meet Federal Aviation Administration (FAA) recommendations in order to upgrade their Runway End Safety Areas (RESAs). In the previous studies, not enough investigations are dedicated to predicting the behavior of the aircraft and its deceleration rate after interfering EMAS and how different materials as arrestor beds would modify aircraft braking distance in RESA. Therefore, secondary objective of this paper is to determine the most optimum height of EMAS slabs, in function of execution costs and accident severity reduction rate. In this regard, a MATLAB®-based numerical code, which simulate the tire-pavement interface, is developed in order to evaluate the functionality of EMAS for aircraft ground maneuvers. Although this code is developed for both dry and wet runway conditions, dry runway's surface is selected as the boundary condition of this study. It simulates aircraft arresting distance by calculating a dynamic skid resistance between aircraft main gear and runway pavement with a fix time step. The results are plotted as risk contour intervals on the layout of EMAS that is installed at the RESA. In addition, this numerical code is adopted in order to perform a sensitivity analysis on five arresting bed materials, which consist of three low-density concretes with maximum crushing stress thresholds of 172500, 345000 and 930000 Pa, one gravel-based material and one foam aggregate-based mixture. Among all, low-density concrete with the highest crushing strength causes shorter aircraft arresting distance.

* Corresponding author.
E-mail addresses: misagh.ketabdari@polimi.it (M. Ketabdari), emanuele.toraldo@polimi.it (E. Toraldo), maurizio.crispino@polimi.it (M. Crispino), vardhman.lunkar@polimi.it (V. Lunkar).

https://doi.org/10.1016/j.cscm.2020.e00446

1. Introduction

Aircraft ground operation events assigned to the runway are classified according to their location of occurrence. Therefore, they can be divided into incursion and excursion events. Runway overruns (in particular, those that occur in landing phase of flight) are responsible for the major portion of runway excursion events. Numerous boundary conditions can convert a normal landing operation into an overrun event (e.g. poor aircraft braking potential conditions due to its low maintenance level, unfavorable weather conditions and pilot errors).

In order to mitigate the severity of consequences of runway overrun incidents/accidents and to protect involved passengers, specific areas after runway end borders are considered which are called Runway End Safety Areas (RESAs) [1]. International Civil Aviation Organization (ICAO) recommended to increase the length of standard RESA from 90 m to 240 m, starting from the end of the runway strip (which itself is 60 m from the end of the runway) [2]. This new dimension is recommended for designing new runways and the existing ones. Although this strategy may mitigate the severity of incidents/accidents, not all the airports have enough land to accommodate these standard recommendations.

The materials beyond the RESA are usually grass or soil with complicated behavior in their arresting capability because their properties are sensitive to weather conditions (such as humidity, temperature, etc.). In wet condition these materials can cause the aircraft to mire down quickly posing a potential for landing gear collapse which can lead to further aircraft damage, therefore, increasing the probability for passenger and crew injury as well as abrupt and consequential fire.

Engineered Materials Arresting System (EMAS), which is approved by Federal Aviation Administration (FAA) [3], is an alternative mitigation strategy for the consequences of landing overrun events for those airports with land-locked circumstances. Therefore, there is no necessity to resize the length of a runway or declare its length to be less than the actual length if there is an adverse operational influence on the airport. In the other word, an adverse operational influence can be the inability of the airport to accommodate its current or planned aircraft fleet.

EMAS is defined as a bed of pre-cast blocks, which can be made of different types of materials as long as complies the FAA requirements, that is placed at the end of a runway to decelerate an overrunning aircraft in an emergency. No external energy source is required for this system since it is a passive mitigation action. These blocks will predictably crush under the weight of an aircraft to provide one gentle aircraft deceleration. Drag forces develop at the tire-arrestor material interface to decelerate the aircraft. The successful deceleration reduces stopping distance considerably. An EMAS requires a highly crushable yet durable material. Therefore, a low-density concrete can be incorporated in the EMAS design. The EMAS is designed to minimize aircraft stopping distance without inducing a detrimentally high inertia force on aircraft passengers or causing major damage to the aircraft landing gear. An EMAS is positioned within the RESA set back area that is located after the runway end border and this setback length protects the arrestor bed from the aircraft intrusion during an under shoot, a short overrun, or material degradation due to jet blast.

FAA includes preliminary EMAS design guides according to aircraft type (e.g. DC-9, DC-10, B737−400, B757, B747, CRJ-200, and G-III) [4] and based on maximum aircraft take-off weight [3]. These guides are used for preliminary EMAS length estimates; however, an actual EMAS can be designed by adopting validated method developed by FAA [4]. Three equations are used to describe the aircraft behavior as it enters through the EMAS:

- Force equilibrium in horizontal direction;
- Moment equilibrium at the aircraft center of gravity in vertical direction;
- Force equilibrium along the strut axis at each landing gear [5].

The basic concepts for modelling the aircraft tire-arrestor material interface to determine the aircraft behavior within the EMAS, are developed based on the previous studies in this field [6].

1.1. Background, literature review and scope

According to the annual reports of Airbus and Boeing, the number of accidents have a decreasing trend for over the last 30 years. In a survey by FAA on the accidents that have occurred in the United States from year 1978 to 1987, that covers only U.S commercial take-off and landing events, approximately 500 events were registered [7]. Out of these 500 records, 246 events were assigned to runway operation accidents, as presented in Fig. 1.

In another similar study, only overrun events that occurred in Australia, Canada, United Kingdom and United States have been investigated, between the years 1980–1998 [8]. Out of the 180 commercial aircraft events, 137 events (76 %) occurred during landing and 43 events (24 %) occurred during take-off. ACRP also examined overrun and undershoot events to compile a worldwide database [9]. 459 events are recorded between years 1982 and 2006, as presented in Fig. 2.

According to these studies, landing overrun can be considered as most probable runway excursion event. Aircraft category, braking potential, weather condition, runway dimensions, runway surface treatment (grooved, porous friction surface), time interval between sequential operations and pilot judgement can affect the frequency of landing overrun events [10]. According to FAA, for 90 % cases of overrun, the aircraft exceeds the runway end at 70 Knots or less and mostly stop within 306 m from the extended runway centerline. Therefore, 306 m long RESA is recommended by FAA to provide enough braking space for aircraft with 70 knotspeed [4], similar to 300 m of a standard RESA length that recommended by ICAO [2], as depicted in Fig. 3.

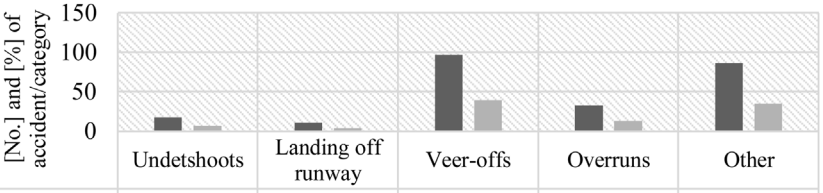

	Undetshoots	Landing off runway	Veer-offs	Overruns	Other
No. of accidents/category	18	11	97	33	87
Percentage of accidents	7.32	4.47	39.43	13.41	35.37

Fig. 1. Number and percentage of accidents for each type of runway-related event [7].

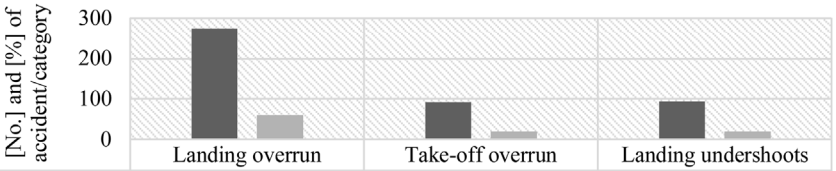

	Landing overrun	Take-off overrun	Landing undershoots
No. of accidents/category	274	92	93
Percentage of accidents	59.69	20.04	20.26

Fig. 2. Number and percentage of accidents for each type of runway-related event [9].

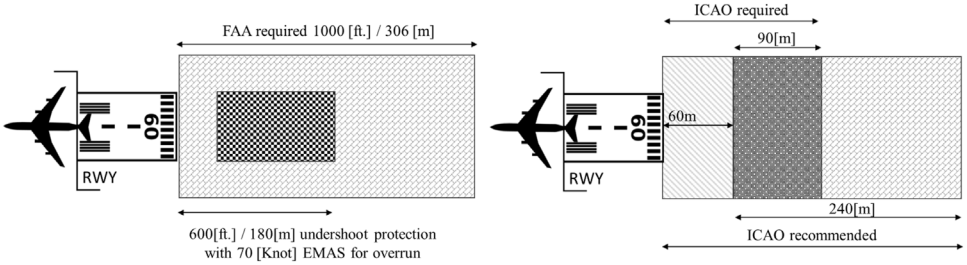

Fig. 3. FAA respect to ICAO recommendations for a standard RESA [2,4].

In order to respect these recommendations, RESA must be capable of supporting the aircraft in occasional overruns, in dry pavement condition, without causing aircraft structural damage or injury to its occupants [11]. It is impossible or impracticable for some airports to achieve to this standard RESA dimension, especially those constructed prior to the adoption of the new requirements of FAA and ICAO, where the airport is surrounded by land constraints (e.g. residential areas, cliffs, mountains, water, etc.).

For these land-locked airports, ICAO provided other alternatives in order to have respect the recommended RESA dimension that can mitigate the severity of landing overrun incidents/accidents [12]:

- Constructing new or enlarging the existing RESA;
- if not possible, modifying or relocating the runway (adding displaced threshold);
- if not possible, installing appropriate arresting system.

Therefore, this study is dedicated to developing a numerical methodology in order to evaluate the behavior of aircraft after entering an installed arresting system (in particular, EMAS) in land-locked airports. According to the literature, some studies made attempts in order to evaluate new materials to be used in construction of EMAS pre-cast blocks. The progress of these existing attempts is given in the following.

In 1985, soft ground arrestor materials (such as clay, sand and water ponds) were considered in designing an arresting bed in order to evaluate their capability in stopping the aircraft in the shortest distance. Investigation was carried out for these materials at their best performance conditions to determine their functionality. The arresting bed simulations indicated that in clay and sand, the stopping distance would be 198 m (650 ft.) and 183 m (600 ft.) respectively. For water ponds, aircraft deceleration would not be neither constant nor gentle, therefore the damages to the aircraft would be more severe. In any case, due to the limitations due to the characteristics of these materials, they were discarded [13].

In 1986, the ARRESTOR computer code was used by FAA to predict aircraft stopping distances after entering RESA [6]. This code is an extension of the FITER 1 which was developed in 1985 by Cook [14] to predict fighter plane movements on soft

ground. The Arrestor code uses EMAS geometry and material properties, and limited aircraft characteristics. This code could analyze the behavior of arrestor for only three types of aircraft - Boeing 707, 727 and 747. In order to evaluate other types of aircraft, a new computer code, SGAS (Soft Ground Arresting System) was developed in 1987 [13]. Though it did not have user friendly pop-up windows, it required the input of only those aircraft parameters which are involved during the tire-material Interaction. The outputs of these programs are the stopping distance, deceleration pattern, gear loads, tire penetration and the EMAS deformation. The sensitivity analysis with the aircraft type showed that the stopping distance increases for the heavier aircraft. The stopping distance increases as the material strength is increased and for a higher bed depth configuration, the aircraft decelerates faster because of the increase in the drag force.

In 2013, four different types of aircraft (B737−900ER, B767−400ER, B757−300, B747−400ER) were investigated. The SGAS that was used for the computations of these aircraft categories, was not included in the FAA arrestor code. Furthermore, sensitivity analysis was carried out considering different EMAS configurations and compressive strength of the material [15]. Typically, an EMAS is designed for the most critical (i.e. heaviest) aircraft operating at the airport.

In 2016, lightweight regional jets have been investigated [16]. Aircraft behavior after entering an installed EMAS at the RESA for CRJ200ER, B727−100, and B737−900ER aircraft have been studied.

The scope of this study is to evaluate the functionality of EMAS in mitigating the possible consequences of landing overruns with the principal aim of safety for the passengers on board. Different arresting bed materials, pre-cast blocks thicknesses and aircraft categories are investigated in order to analyze the sensitivity of each parameters on the aircraft braking distance.

2. Research method: aircraft behavior within an EMAS

Aircraft behavior within the EMAS area, can be analyzed by aircraft stopping distance. This distance in landing overrun can be defined as the distance from the runway end at which the aircraft decelerates to a complete stop within the EMAS [17]. The maximum EMAS entry velocity is based on the system design requirements laid down by the FAA and it is 70 Knots or 36 m/s. the approach to simulate the aircraft behavior inside the EMAS is based on Probabilistic Risk Analysis (PRA). Therefore, aircraft touchdown velocity is considered into the simulation as a normal Probability Density Function (PDF).

2.1. Aircraft stopping distance

A numerical approach is implemented in MATrix LABoratory (MATLAB®) in order to compute the stopping distance of the aircraft within different EMAS materials. The input parameters, which can be collected from the airport planning manuals for each type of aircraft, are: aircraft Maximum Landing Weight (MLW), wing area *(A)*, tire radius *(R)*, tire width *(S)*, tire deformation (δ_t), air density (ρ), coefficient of drag (C_D) and lift (C_L) for the concerned aircraft, and EMAS entry velocity normal distribution. The dimensionless coefficient of lift relates the lift generated by a lifting body to the fluid density around the body. The fluid velocity and an associated reference area, can be calculated by Eq. (1) [18]:

$$C_L = 2 \times MLW \times g/(\rho \times V^2 \times S) \tag{1}$$

Where, *MLW* is maximum landing weight of the aircraft [kg]; g is acceleration due to gravity [m/s^2]; ρ is air density [kg/m^3]; V is aircraft cruise speed [m/s]; and S is aircraft wing area [m^2]. C_D, which is used to quantify the drag or resistance of an object in a fluid environment, such as air or water, is calculated from C_L by Eq. (2) [19]:

$$C_D = C_d + C_L^2/(AR \times \pi \times e) \tag{2}$$

Where, C_d is coefficient of drag at zero lift, which for light aircraft can be from 0.02 to 0.04 and for subsonic aircraft can be from 0.013 to 0.020; AR is aspect ratio of the concerned aircraft; and e is shape efficiency factor that for rectangular foils 0.7 is selected.

Aircraft behavior in five types of arrestor material, with various mass densities (ρ), is simulated and investigated in order to determine a material with better functionality to be used in pre-cast blocks. These materials consist of three low-density concretes with maximum crushing stress levels (P_C) of 172500, 345000 and 930000 Pa, one gravel-based material and one foam aggregate-based mixture. The main objective of adopting different materials in the simulation is to evaluate the functionality of low-density concretes with different crushing strengths, meanwhile, gravel and foam aggregates are also adopted in order to express in a clearer way the impact level of different types of materials on the functionality of EMAS. Low crushing stress level causes low durability for the concrete which can be an issue in maintenance of EMAS infrastructure. Selection of low-density concretes with various crushing stress levels does not confirm that they are economical materials to be adopted for EMAS since this statement needs corresponding cost-benefit analysis. Therefore, low-density concretes with 172500 Pa and 930000 Pa crushing stress levels are adopted in order to study the behavior of EMAS materials with lowest and highest crushing strength. Fig. 4 presents typical low-density crushable concrete behavior. The concrete exhibits a strain increase as stress increases. Beyond yielding, the material exhibits a large strain increase at a nominally constant stress (within 0.2 to 0.5 strain range). Beyond 0.5 strain, additional stress is required to develop larger strains. As the material approaches a fully crushed state (0.8 strain), a substantial stress increase is required to develop marginal strain increases.

The behavior of gravel and foam aggregate are constant and their related crushing stresses and mass densities are presented in Chapter 4.

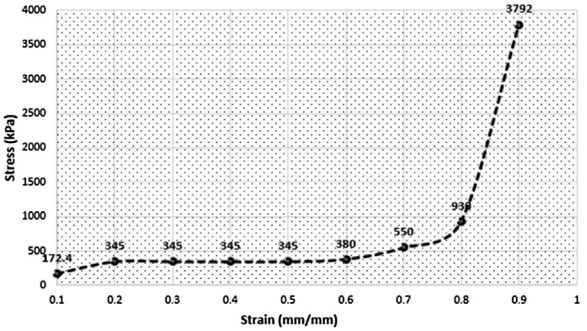

Fig. 4. Low-density concrete stress/strain relationship [20].

Another fundamental input in the computation is the dimension of EMAS precast blocks in terms of length, width and thickness, which form the entire arrestor bed. Therefore, instead of introducing each precast concrete, it is possible to insert the dimension of the entire arrestor bed as input into the calculation. The width of the EMAS is necessary since it should cover the longest Outer Main Gear Wheel Span (OMGWS) of the critical aircraft. Moreover, solver parameters (e.g. discretization of time, probability bar interval and the properties of touchdown normal PDF) are required to be considered in the numerical computation.

2.2. Conceptual model to determine drag and vertical forces from tire-material interface

As an aircraft enters an arresting bed, material crushes under the aircraft's self-weight and creates an interface between the tire and arresting material. The forces that are generated at the interface are vertical force, which supports the aircraft weight, and drag force, which aids in aircraft deceleration. For this matter, a conceptual model [13] is implemented to involve these forces into principal equilibrium of deceleration rate and consequent arresting distance simulations. EMAS entry velocity is inserted in the calculations as normal Probability Density Function (PDF), but MLW of aircraft are considered in the computation in order to study the worst-case scenario (critical events). Therefore, for each type of aircraft, the corresponding MLW is adopted instead of a PDF of weight.

The tire-material interface model is required to couple the forces generated as the result of confronting arresting material and aircraft landing gear. Consequently, deceleration rate, drag and vertical forces and ultimately stopping distance can be obtained. The drag and the vertical forces are functions of material mass density, crushing stress, EMAS entry velocity, and tire footprint area. In other words, vertical and the drag forces are equal to the pressures on the horizontal (A_W) and vertical tire footprints (A_F), as shown in Fig. 5.

Tire deformation has dynamic characteristic and it changes according to the velocity of the aircraft that leads to variation in tire footprint [21].

A probabilistic code is implemented in MATLAB® software in order to simulate the aircraft behavior after entering different EMAS materials. Various boundary conditions such as weather parameters, water-film thicknesses, MLWs, and touchdown speed PDFs are assigned into the computations. The computation strategy is explained in continue:

$$F_D = \underbrace{0.5pAV^2C_D}_{\text{Aerodynamic Drag Force}} + \{\underbrace{(Pc + 0.5P_cV^2)}_{\text{Crushing Strength + Dynamic Stress as a function of entry Velocity of Aircraft}} \times \underbrace{S \times (Z_M - \delta_t)}_{\text{Projected Area of the Tire (A}_F\text{)}}\} \times C_d \quad (3)$$

$$Fv = \underbrace{0.5pAV^2C_L}_{\text{Aerodynamic Lift Force}} + \{\underbrace{(P_c + 0.5P_cV^2)}_{\text{Crushing Strength + Dynamic Stress as a function of entry Velocity of Aircraft}} \underbrace{S \times W \times 0.66}_{\text{Projected Vertical Area (Aw)}}\} \times C_L + \underbrace{K \times \delta_t}_{\text{Vertical Spring Force}} \quad (4)$$

$$W = R^2 - (R - Z_m + \delta_t)^2 - R^2 - (R - \delta_t)^2 \quad (5)$$

Where, A is the aircraft wing area [m^2]; R is landing main gear radius [m]; S is tire width [m]; δ_t is the tire deformation; ρ is the air density [kg/m^3]; C_D is the coefficient of drag; C_L is the coefficient of lift for the concerned aircraft; Z_M is EMAS thickness

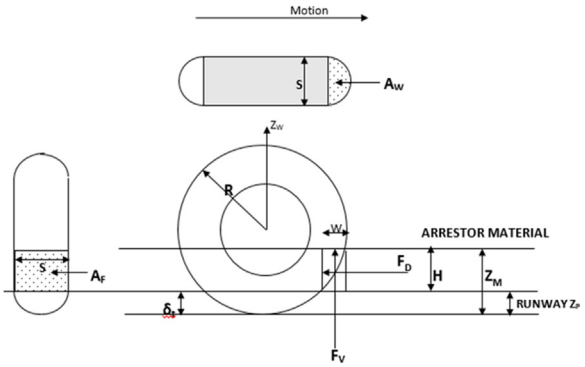

Fig. 5. Wheel interface model to define drag and vertical forces [13].

[m]; P_c is the material crushing stress [Pa]; F_D is the generated drag force; F_V is the generated vertical force; W is the main gear foot print after entering the EMAS area.

Induced drag and vertical forces can be computed by Eqs. (1),(2) and (3), and these values are adopted in the equation of Equilibrium of Newton's Second Law in order to compute the aircraft deceleration rate.

$$\frac{F_D}{MLW} + M_c \times (g) - \frac{M_c \times (F_V)}{MLW} = a \tag{6}$$

Where, a is the aircraft acceleration rate [m/a^2]; M_C is coefficient of friction between the tire and arrestor material; MLW is maximum landing weight of the aircraft [kg].

Stopping distance can be then calculated by the following equations:

$$S = \int_0^t V(t)dt = \sum_i (\Delta Xi) \tag{7}$$

$$V(t) = V(t=0) - \int_0^t a(t)dt \tag{8}$$

$$V(T) = 0 \tag{9}$$

Where, $V(t)$ is aircraft speed at time t. t_0 is the time when the aircraft brakes are first applied; T is the time at which the aircraft comes to a complete stop, that is $V(T) = 0$; ΔX is the distance covered over time interval Δt; and $a(t)$ is deceleration rate of aircraft at time t [13].

Thus, an incremental distance and a new reduced speed due to deceleration is computed at every step which becomes the initial conditions for the computations in the next step. The distances are added cumulatively to get the final stopping distance when the aircraft comes to a complete stop. So, the computation continues till the EMAS entry velocity reaches a zero at final time.

This numerical computation is compatible with multiple wheels and dual-gear airplanes.

3. EMAS application for a regional jet CRJ 200 ER

An illustrative example for application of the numerical code is made in this chapter. A regional jet (CRJ200-ER) is selected in the computation to evaluate the aircraft behavior and its final stopping distance after entering EMAS for a runway with average length of 2000 m. The selected EMAS length, width and thickness are 100, 60 and 0.3 m respectively and the material of the EMAS is selected as low-density concrete with crushing (threshold) stress Pc, 345 kPa. Pc is the ultimate stress at which the highest strains are produced and after which greater stresses are required to increase the marginal strains.

General Aviation with Maximum Take Off Weights (MTOW) less than 5.7 t will normally stop within the selected length interval of runway without entering EMAS area, therefore, mainly commercial aircraft (with MTOW $\geq$ 5.7 t) are considered in order to study the behavior of EMAS. Assumptions that are considered in order to develop this application are as following:

- Reverse thrust is not being considered as the aircraft exits the runway;
- There is minimal or no structural damage to the landing gear;

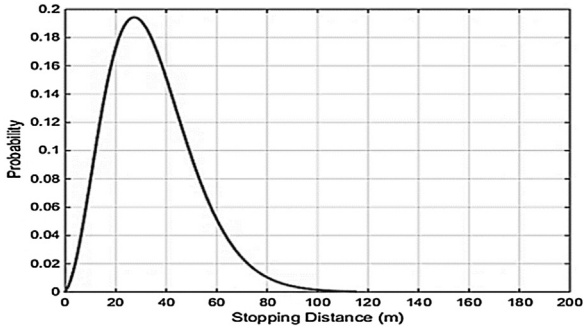

Fig. 6. Achieved output: Aircraft arresting distance PDF (CRJ200-ER).

- Aircraft braking system is in well-maintenance condition;
- There is no aircraft braking or use of reverse thrust once an aircraft enters the EMAS area.

Fig. 6 shows the probability distribution of aircraft arresting distance, as an output of the simulation. Since EMAS entry velocity is inputted as a normal PDF, the output of aircraft arresting distance is also in form of PDF. The peak of the PDF is demonstrating that it is more probable for this aircraft to reach to the final stop before 25 m from entering the EMAS. Although for the selected length of the EMAS in this application is 100 m, according to real practices of EMAS installations in several airports, the typical length of EMAS area is 60 m, which by referring to Fig. 6 it can be a proof for the arresting bed functionality.

The tail of this PDF (extreme rare scenarios) indicates that there is still a low probability that the aircraft passes the EMAS end and causes consequences.

Cumulative arresting distance PDF for CRJ200-ER regional jet is presented in Fig. 7a. It can be observed that the probability accumulates faster till 80 m from the EMAS entry and then changes slightly till the full arresting distance.

Mean stopping distance PDF is depicted in Fig. 7b. At every step, a mean arresting distance from the EMAS entry is computed and it is displayed in the form of a discrete PDF.

These PDFs are implemented in developing the final probability contour intervals.

Variation of drag and vertical forces with the probability of aircraft arresting distances are presented in Fig. 8a. The results show that there is non-linear relationship between the drag and vertical forces and aircraft arresting distances. As the aircraft overruns the runway end and enters the EMAS, the drag force develops at the tire-arresting bed interface which helps in decelerating the aircraft. As the aircraft move forward through the arresting bed, drag force increases, till the aircraft comes to a full stop.

An EMAS is positioned within the RESA. It is positioned within the Runway Safety Area (RSA), sets back from the runway threshold and this setback length protects the bed from aircraft intrusion during an under shoot, EMAS entry during a low velocity overrun and material degradation due to jet blast. Upon the available area at the RESA and the selected material of the EMAS this setback distance may be vary. Therefore, to plot the results, stopping distance zero is related to the starting point of aircraft entering the EMAS materials.

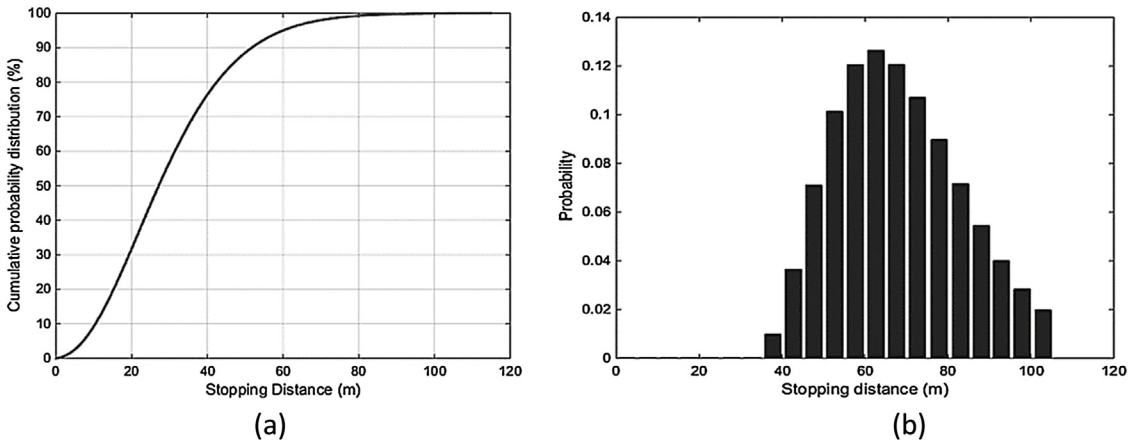

Fig. 7. Achieved outputs: (a) Cumulative PDF, (b) Mean aircraft arresting distance PDF.

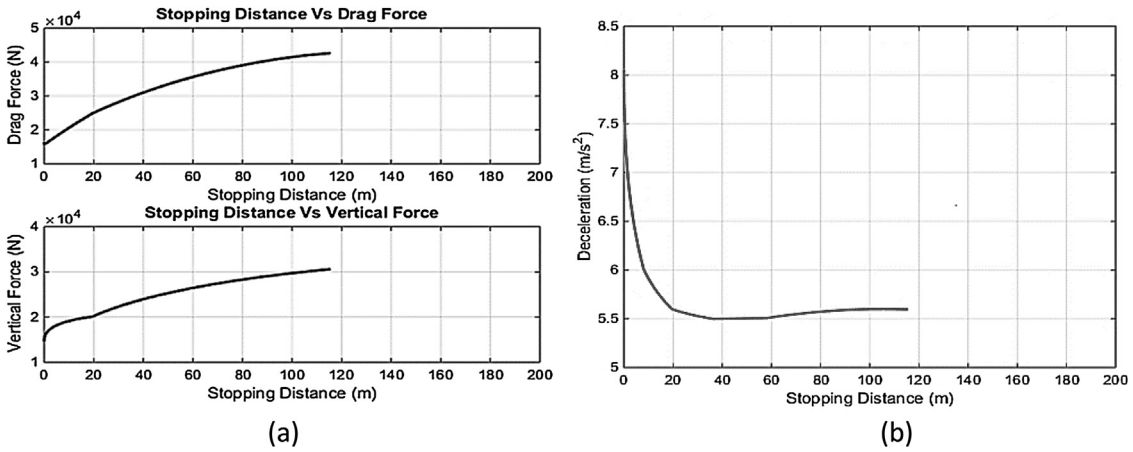

Fig. 8. Achieved outputs: (a) Drag and vertical forces and (b) Deceleration rate, versus aircraft arresting distances.

The relation between deceleration rate and aircraft arresting distance is depicted in Fig. 8b. Initially there is a high deceleration rate due to the EMAS entry due to the friction properties of the material. But afterward, as the aircraft velocity decreases, the deceleration rate also decreases. The aircraft gently decelerates (almost with a constant deceleration rate) till it comes to a full stop.

Since deceleration rate is directly proportional to the velocity of the aircraft, where velocity decreases the deceleration rate is also decreases. Probabilistic contour intervals of aircraft arresting distances, as the final output, is basically a representation of the spatial probability distribution of aircraft arresting distances within the EMAS bed, that is plotted at the end of the under-study runway. This output determines critical locations on the EMAS geometry with higher probabilities of aircraft full stop. The calculated arresting distances contour intervals for CRJ200-ER regional jet is presented in Fig. 9.

According to Fig. 9, the average probabilities of arresting distances (in term of percentage) are higher in the vicinity of the EMAS entry origin. It is more probable that CRJ200-ER stops before 80 m from the entry origin. The probability the CRJ200-ER overrun the total EMAS area is 4.3 % (2.5 % + 1.8 %) beyond 100 m, which means in 95.7 % of the landing overrun events EMAS can arrest an overrunning CRJ200-ER without any catastrophic consequences.

4. Sensitivity analysis on different arrestor materials

The behavior of CRJ200-ER regional jet after entering the EMAS is investigated for different arrestor bed materials with their specific crushing strengths and mass densities. As explained earlier in Fig. 4, in low-density concretes, the strain

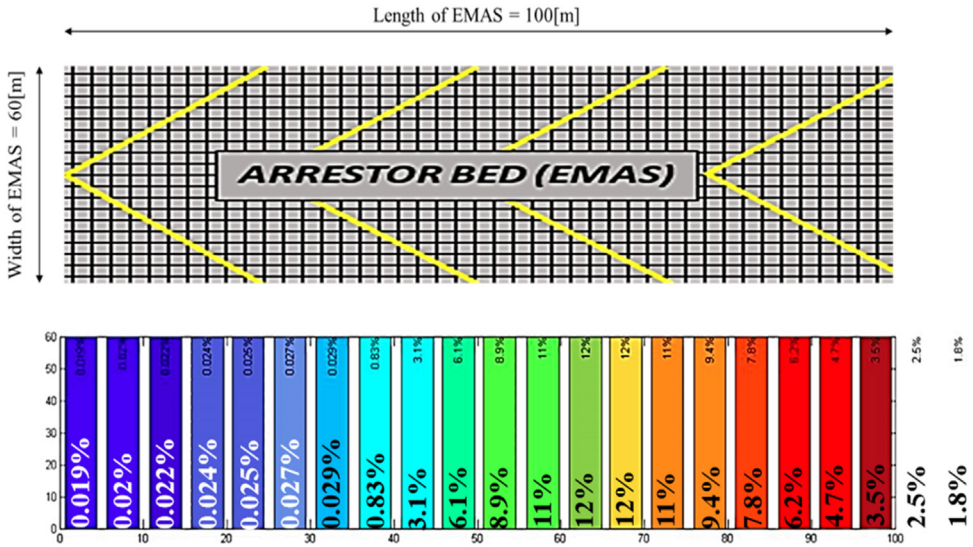

Fig. 9. Achieved output: Probabilistic contour intervals for CRJ200-ER arresting distances.

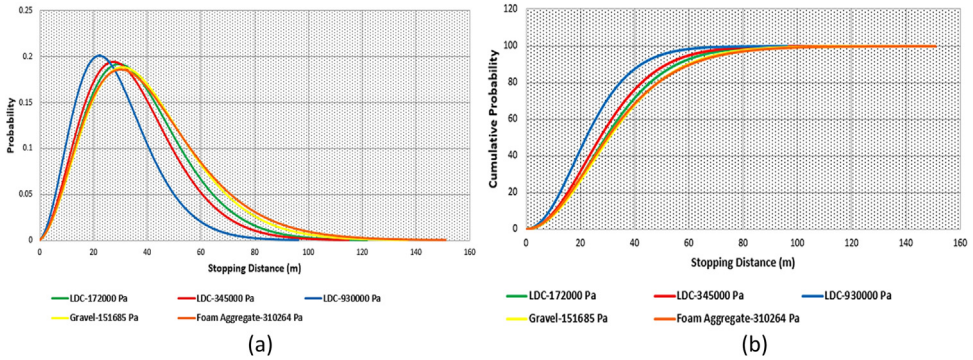

Fig. 10. (a) CRJ200-ER arresting distance PDF, (b) Cumulative PDF for different materials.

increases initially respect to low variation in the stress values but after the material yield stress, there is a significant increase in stress but limited in strain values. Therefore, low-density concretes are investigated to evaluate the behavior of aircraft after entering the EMAS area and to determine the relation between the arresting distances and type of materials.

It can be observed from Fig. 10a that among the low-density concrete mixes, there is a decrease in the aircraft arresting distance by increasing the crushing stress of the material. The arresting distance is maximum for the foam arrestor bed because of its extremely low mass density due to which a very low drag force is generated at the tire-material interface. Therefore, the aircraft travels a longer distance before coming to a full stop.

Arresting bed consists of gravel also leads to longer arresting distance because of its low crushing strength. It means, the drag force induced by the material has a correlation with the material's crushing strength and its mass density. The greater crushing strength material manages to exert, the greater drag force against the landing main gear will be generated, consequently aircraft reach to a full stop at a shorter distance, as presented in Table 1. The foam arrestor bed induces least drag force on the landing main gear due to its extremely low mass density, as shown in Fig. 11a.

Table 1
Selected arresting bed materials with their properties.

No.	Arrestor materials	Mass density [kg/m^3]	Crushing stress [N/m^2]	Arresting distance [m]	Maximum drag force [N]
1	Low-density concrete A	2300	175000	121.9	38800
2	Low-density concrete B	2300	345000	114.8	42600
3	Low-density concrete C	2300	930000	96.1	55470
4	Gravel	1680	151685	137	25000
5	Foam aggregate	176	310264	151	12000

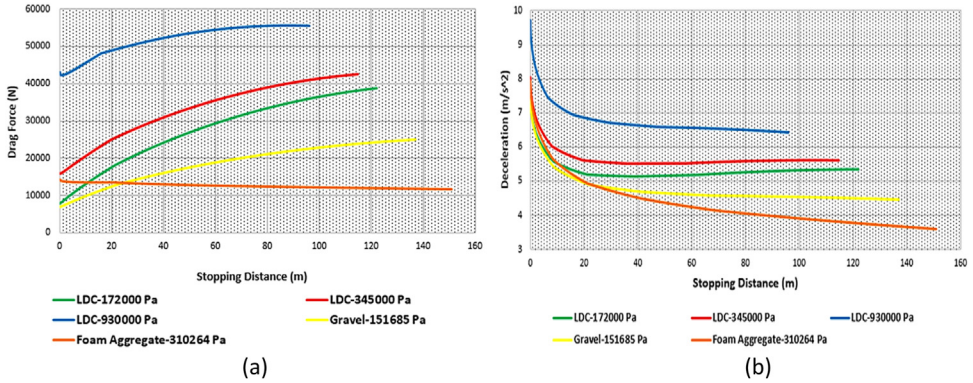

Fig. 11. (a) Generated drag force, (b) CRJ200-ER deceleration rate for different materials.

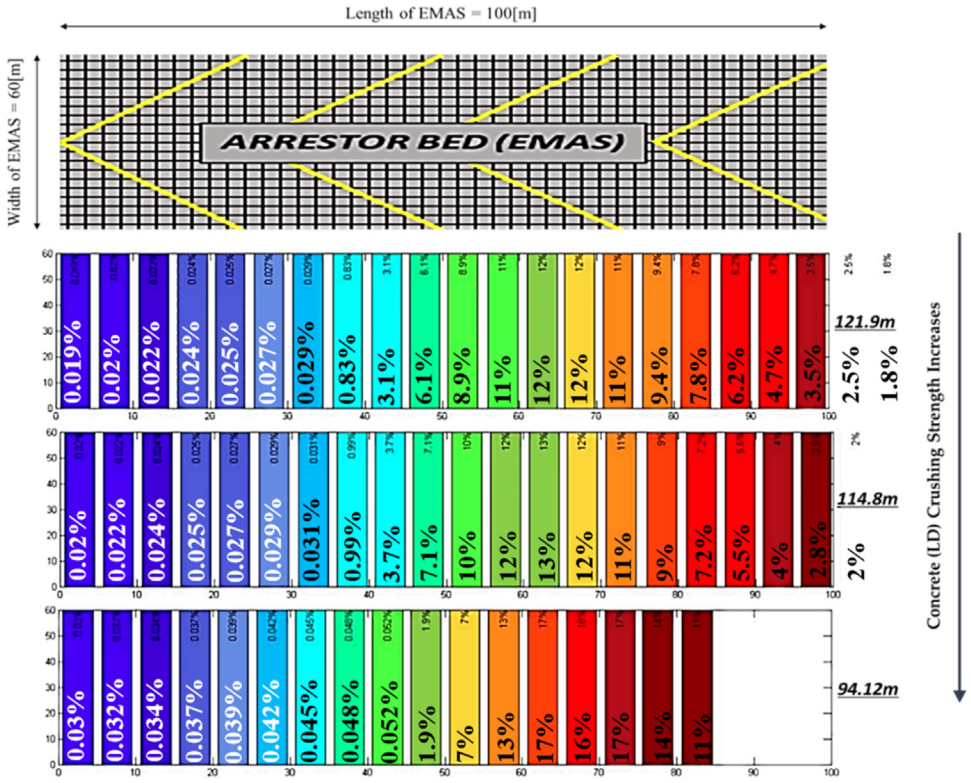

Fig. 12. Contour intervals for low-density concrete mixes (crushing strengths 172500, 345000 and 930000 Pa).

It can be observed from Fig. 10b, that how the cumulative PDF of arresting distances shifts to the right for materials with lower arresting properties. This achievement proves that it is more probable for gravel and foam arresting beds that the aircraft reach to a full stop in a longer distance from the EMAS entry origin compared to low-density concrete mixes.

In materials with higher crushing strength, the CRJ200-ER decelerates faster since higher drag forces are generated, as shown in Fig. 11b.

The calculated arresting distances contour intervals, alongside the arrestor bed configuration (100×60 m), for CRJ200-ER regional jet is presented in Fig. 12.

Material with the highest crushing strength shows the most effective arresting behavior since it generates the highest deceleration rate respect to other materials. As depicted in Fig. 12, the concrete mixes with 172500 and 345000 Pa crushing strengths are in fact failing to decelerate the aircraft within the EMAS considered length (100 m).

5. Sensitivity analysis on different aircraft types and EMAS thicknesses

To explore the functionality of low-density concretes, additional sensitivity analyses are performed based on different EMAS thicknesses and aircraft types. The results are presented in terms of aircraft arresting distances and generated drag and vertical force, during landing overrun events.

5.1. Aircraft type

As the MLW of an aircraft increases, the drag and vertical forces also increase (due to changes in wingspan and main gear dimensions). For this reason, aircraft CRJ200-ER, B727−100, B707−320C and B747−100 are selected for sensitivity analysis of their influence on the arresting distances and drag and vertical forces after entering low-density concrete EMAS materials. The reasons to choose these set of aircraft are;

- FAA implemented the ARRESTOR CODE (before the SGAS code) for these aircraft [13], therefore, verifying the results with the previous studies will be more feasible;
- To have a wider range of aircraft MLWs, covering from regional jets (21390 kg) to B747 (255800 kg) for conducting more comprehensive sensitivity analysis. In fact, the mass is a dominant factor that affects the deceleration rate (inversely

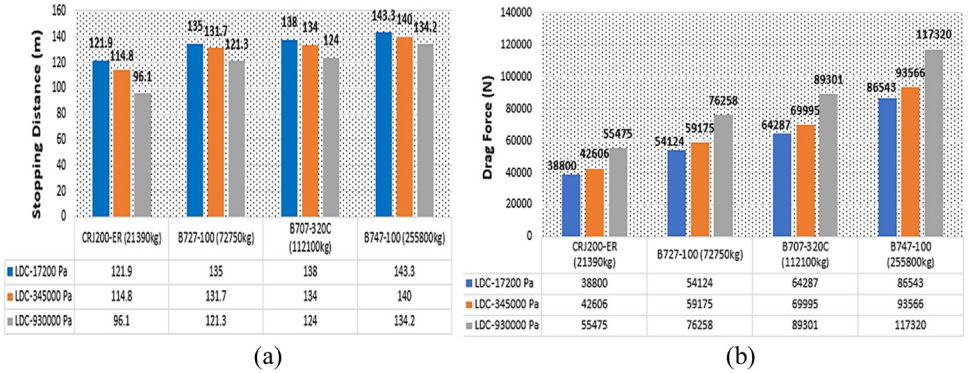

Fig. 13. (a) Arresting distances, and (b) Maximum drag forces for selected aircraft.

proportional) and thus the deceleration rate decreases with the increase in the MLW of an aircraft. This prolongs the final arresting distance, as presented in Fig. 13a;

- CRJ-200 with MLW equal to 21390 kg is still a commercial aircraft and not a GA, Since GA are those aircraft with landing weight less than 5.7 t. Therefore, these for commercial aircraft with different MLWs are selected in order to perform the sensitivity analysis on the behavior of EMAS after aircraft entrance.

As explained earlier, two principle forces that are generated at the tire-arresting material interface are drag and vertical forces. The drag force is responsible for the aircraft deceleration and the vertical force supports the aircraft weight (Fig. 14).

As the aircraft MLW increases the drag force increases due to the variation in aircraft characteristics (e.g. wingspan, main gear size), as shown in Fig. 13b, and the vertical force, which is representing the lift, increases. Since, the lift increases, the aircraft travels a longer distance within the EMAS area. As the material strength Pc (LDC) increases, the aircraft travels shorter stopping distances within the EMAS, as shown in Fig. 13a.

5.2. EMAS thickness

The aircraft arresting distances are evaluated by altering the thickness of the EMAS (Z_m), which is used in the drag formulation. As presented in Fig. 15a, arresting distances for selected aircraft decrease with the increase in the EMAS thickness, since the drag forces also increase, as shown in Fig. 15b.

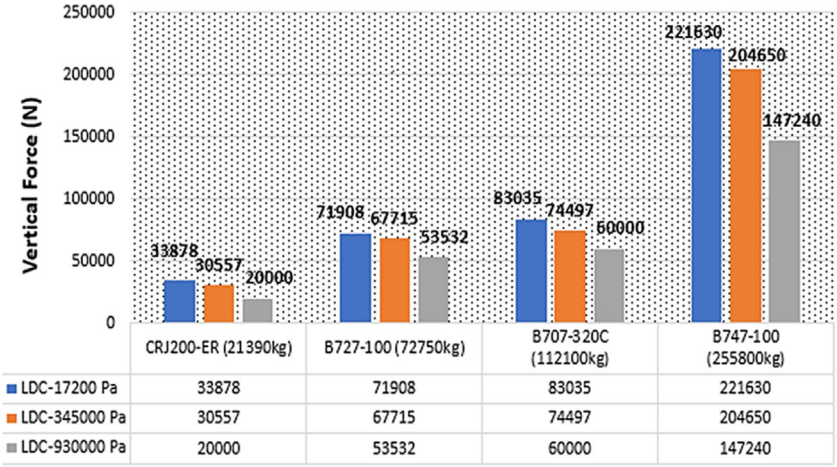

Fig. 14. Maximum vertical forces for selected aircraft.

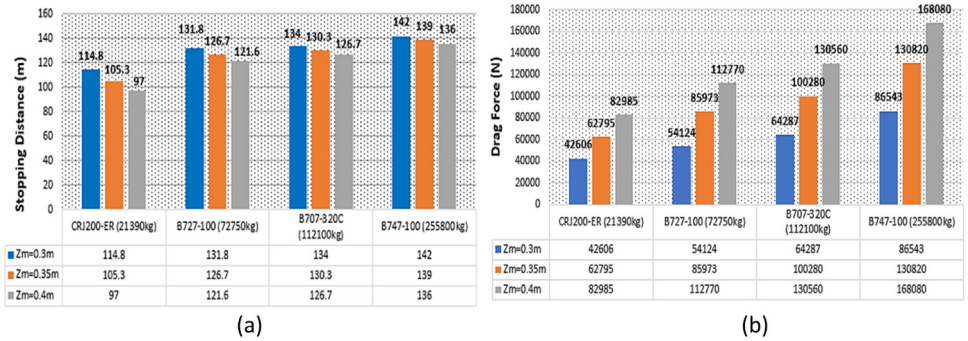

Fig. 15. (a) Arresting distances, and (b) Maximum drag forces as a function of EMAS thickness for selected aircraft.

6. Conclusion

The scope of this study is to evaluate the functionality of EMAS in mitigating the possible consequences of landing overruns with the principal aim of safety for the passengers on board. This risk mitigation approach, which is approved by FAA [3], is an alternative risk mitigation strategy for the consequences of landing overrun events for airports with land-locked circumstances.

In this study, the aircraft behaviors after entering EMAS area are investigated. For this matter, a probabilistic model is implemented in MATLAB® software to compute the aircraft arresting distances within the EMAS area in landing overrun events. In this regard, a conceptual model is adapted from the previous studies, which is upgraded in order to simulate the drag and vertical forces generated at the tire-arresting material interface. Then, based on Newton's second law the aircraft deceleration rate is computed in order to determine the final aircraft arresting distances. The main outputs from this probabilistic code are as follows:

- Aircraft arresting distance PDF after entering EMAS area;
- Relation between EMAS entry velocity and aircraft arresting distance;
- Relation between aircraft decelration rate and arresting distance;
- Relation between drag and vertical forces and arresting distance;
- Cumulative aircraft arresting distance PDF;
- Probability contour intervals of aircraft arresting distances after entering EMAS area.

Aircraft behavior is analyzed for different EMAS materials (low-density concretes, gravel and foam aggregates), aircraft types (CRJ200-ER, B727−100, B707−320C and B747−100) and EMAS thicknesses (0.3, 0.35 and 0.4 m).

Aircraft arresting distance within the EMAS area decreases when the crushing strength of the material increases. Arresting bed formed by foam aggregates material causes the longest aircraft stopping distance because of its extremely low mass density. Gravel bed causes the longer arresting distance respect to low-density concrete mix. The reason attributes to its lower crushing strength.

Drag force has a direct correlation with the material's crushing strength and mass density. Materials with greater crushing strengths cause greater drag forces against the landing gear, therefore, aircraft reaches to a full stop at a shorter distance.

As the aircraft MLW increases, the drag and vertical forces also increase, due to changes in aircraft characteristics (e.g. wingspan and main gear dimension). MLW is a dominant factor that affects the aircraft deceleration rate (inversely proportional). A sensitivity analysis for different EMAS thicknesses is performed in order to analyze aircraft behavior after entering the EMAS area. Aircraft arresting distances decrease with the increase in the EMAS thickness, since the drag force increases.

Outputs of the calculations are plotted as arresting distances contour intervals, alongside the arrestor bed configuration (100×60 m) for low-density concrete mixes (with crushing strength of 172500, 345000 and 930000 Pa). To conclude, an EMAS can be considered as the most rational and feasible alternative solution for land-locked airport in order to respect the FAA and ICAO RESA recommendations and mitigating the consequences of landing overrun events.

Data availability

The processed data required to reproduce these findings are available to download from [https://data.mendeley.com/datasets/f5tmsfpwrm/1] with DOI: 10.17632/f5tmsfpwrm.1.

Declaration of Competing Interest

The authors report no declarations of interest.

Acknowledgement

This research did not receive any specific grant from funding agencies in the public, commercial, or not-for-profit sectors.

References

[1] Study on Models and Methodology for Safety Assessment of Runway End Safety Areas", European Aviation Safety Agency, Final report, 2014.
[2] Operation of Aircraft - International Commercial Air Transport – Aeroplanes, International Civil Aviation Administration, ICAO Annex 6 - Part 1, 2010.
[3] Financial Feasibility and Equivalency of Runway Safety Area Improvements and Engineered Material Arresting Systems, FAA Order 5200.9, 2004.
[4] Engineered Materials Arresting Systems (EMAS) for Aircraft Overruns, FAA Advisory Circular 150/5220-22A, 2005.
[5] E. Heymsfield, W.M. Hale, T.L. Halsey, Aircraft response in an airfield arrestor system during an overrun, J. Transp. Eng. 138.3 (2012) 284–292.
[6] E. Heymsfield, Performance Prediction of Strong Company's Soft Ground Arrestor System Using a Numerical Analysis, Mack Blackwell Transportation Center, Arkansas, USA, 2009.
[7] R.E. David, Location of Commercial Aircraft Accidents/Incidents Relative to Runways (No. DOT/FAA/AOV-90-1), Federal Aviation Administration Washington DC, 1990.
[8] I. Kirkland, R.E. Caves, M. Hirst, D.E. Pitfield, The normalisation of aircraft overrun accident data, J. Air Transp. Manag. 9 (6) (2003) 333–341.
[9] J. Hall, M. Ayres, D. Wong, Analysis of Aircraft Overruns and Undershoots for Runway Safety Areas, Airport Cooperative Research Program Rep. 3, Transportation Research Board, Washington, DC, 2008.
[10] M. Ketabdari, F. Giustozzi, M. Crispino, Sensitivity analysis of influencing factors in probabilistic risk assessment for airports, Saf. Sci. 107 (2018) 173–187.
[11] M. Crispino, E. Toraldo, F. Giustozzi, Improving runway strip performance to fulfill international requirements through eco-efficient soil treatments: case study of a major italian airport, Environ. Engin. Manage. J. (EEMJ) 17 (6) (2018).
[12] International Civil Aviation Administration, ICAO, 6th ed, Annex 14: Aerodromes – Aerodrome Design and Operations, Vol. 1, Convention on international civil aviation, 2013.
[13] R.F. Cook, Soft-Ground Aircraft Arresting Systems, Universal Energy Systems Inc Dayton OH, 1987.
[14] R.F. Cook, Aircraft Operation on Soil Prediction Techniques, Technical Report ESL-84-04, Vol. 1 and 2, U.S, Air Force Engineering and Services Centre, Tyndall Air Force Base, FL, 1985.
[15] E. Heymsfield, Predicting aircraft stopping distances within an EMAS, J. Transp. Eng. 139 (12) (2013) 1184–1193.
[16] E. Heymsfield, Jet stopping distance and behaviour in a regional airport EMAS, J. Perform. Constr. Facil. 30.5 (2016)04016010.
[17] M. Ketabdari, M. Crispino, F. Giustozzi, Probability Contour Map of Landing Overrun Based on Aircraft Braking Distance Computation, Pavement and Asset Management, CRC Press, 2019, pp. 731–740.
[18] L.J. Clancy, Aerodynamics, Halsted Press, 1975.
[19] L.K. Loftin, Quest for Performance: the Evolution of Modern Aircraft (No. 468), Scientific and Technical Information Branch, National Aeronautics and Space Administration, 1985.
[20] E. Heymsfield, T.L. Halsey, Sensitivity analysis of engineered material arrestor systems to aircraft and arrestor material characteristics, Transp. Res. Rec. 2052 (1) (2008) 110–117.
[21] H.R. Pasindu, T.F. Fwa, Ghim Ping Ong, Computation of Aircraft Braking Distances, Transportation research record 2214.1, 2011, pp. 126–135, doi:http://dx.doi.org/10.3141/2214-16.